Development of Potent SARS-CoV 3CL Protease Inhibitors: *In silico* Analogues Designing of Darunavir, Molecular Modelling and Molecular Dynamic Simulation

MAHWISH AKHTAR[1,] , NOOR JAHAN[2,] , MUHAMMAD IMRAN[3,*,] , SALMAN ASHFAQ AHMAD[3,] ,
SARA NAQVI[3,] and SYED MUHAMMAD HUZAIFA SHAH[4,]

[1]Department of Pharmaceutical Chemistry, Faculty of Pharmaceutical Sciences, Dow College of Pharmacy, Dow University of Health Sciences, Karachi, Pakistan
[2]Department of Pharmacology, Faculty of Pharmaceutical Sciences, Dow College of Pharmacy, Dow University of Health Sciences, Karachi, Pakistan
[3]Department of Pharmacy, Iqra University, Karachi, Pakistan
[4]Medical College, Ziauddin University, Karachi, Pakistan

*Corresponding author: Tel.: +92 333 7532242; E-mail: muhammad.imran2409@gmail.com

COVID pandemic initiated in early 2019 and the origin from where it initiated was Wuhan city of China. It changed the whole world. A huge population died due to COVID-19 in spite of taking precautions. New treatments and vaccines are introduced for the treatment and prevention. Among successful treatments, antivirals were found effective against COVID-19. But there is a need to find derivatives, which could be more effective for the treatment of COVID-19. The current research is focused on computational studies on one of the antiviral, darunavir. A computational strategy, molecular docking and molecular dynamic simulation techniques is presented to discover the potent analogues of darunavir for inhibiting protease 3CLpro of SARS-CoV2. The newly discovered X-ray structure (PDB ID: 6LU7) was selected for docking study and generated analogues were docked. The docking results showed that the compounds were bound in the active site of receptor with good binding affinity. It was concluded that compounds D8 and D15 were have good binding affinity value of -9.85 and -8.95 kcal/mol, respectively and these compounds were selected for molecular dynamic simulation (MDS) study to check their stability in pocket of receptor.

Keywords: COVID-19, Darunavir, Computational strategy, Molecular docking.

INTRODUCTION

SARS-CoV2 is the cause of COVID-19 in humans. It is pandemic and it has affected a large population of the world. Initially in 2002, SARS-CoV2 was known to cause mild respiratory and gastrointestinal disease [1]. The first human corona virus (HCoVs) were described in 1966, E229-CoV and OC43-CoV. All HCoVs are globally endemic and frequently cause common colds, accounting for 2-18% of all respiratory tract infections [2]. In the immune-compromised patients, infants, the elderly and those with pre-existing pulmonary disorders, HCoVs can cause severe respiratory or sepsis-like presentations [3]. The SARS pandemic of 2002/3 was originated in Foshan, Guangdong province, China and spread to South East Asia, Europe and North America [4]. Common features included were

massive inflammatory cell infiltration of the lungs resulting in acute lung injury (ALI) and acute respiratory distress syndrome (ARDS), highly elevated inflammatory markers in the serum, evidence of monocyte/macrophage activation, activated coagulation and pro-inflammatory cytokine and chemokine profiles [5]. Similar descriptions of clinical presentations in COVID-19 are now emerging like cough and fever, sub-acute progression to respiratory distress and ARDS in 8-19% of patients. The risk of morbidity is greater with elderly patients and those with underlying comorbidities especially cardio-vascular disease, diabetes mellitus, chronic pulmonary disorders or renal disease [6]. The pulmonary pathology in COVID-19 is characterized by diffused alveolar damage, focal reactive hyperplasia of pneumocytes with patchy inflammatory cellular infiltration and evidence of intravascular thrombosis. Monocytes,

macrophages and lymphocytes infiltrate the pulmonary interstitium [7]. In addition, one fifth of hospitalized patients developed significant cardiovascular morbidity, characterized by troponin rise, tachyarrhythmias and thromboembolic events, which led to mortality risk [8]. While an estimated 80% of SARS-CoV2 infections are asymptomatic or result in mild disease, the remaining 20% of patients are severely or critically unwell [9]. Vaccines are developed for the prevention of COVID-19 [10].

Hydroxychloroquine was the first drug used for the treatment of COVID-19. It has immunomodulatory activity and antimalarial and antiinfluenza effect. It is utilized in systemic lupus erythromatosis. It is also effective in Chikungunya virus, seasonal CoVs and SARS [11]. Second drug trialed for SARS-CoV-2 treatemnt was azithromycin. It has immunomodulatory activity and this antibiotic is used for respiratory tract infections, but its reduced mortality rate in the patients [12]. Third treatment trails were started with remdesivir and other nucleoside analogues. Competing with ATP and substituting for adenosine during RNA synthesis, remdesivir inhibits the viral RNA dependent RNA polymerase (RdRp) [13]. Initially remdesivir was used for treatment of Ebola (EBOV) and Marburg viruses (MERS). Combination of lopinavir/ritonavir is also found effective against COVID-19. Proteases are required for maturation of infectious virion, which is inhibited by lopinavir/ritonavir [14]. Recombinant soluble angiotensin converting enzyme 2 (ACE2) is also tested and found as key molecule for cell invasion and its blockade can control disease [15]. SARS-CoV-2 infection inhibits the expression of type 1 interferons. Resulting tissue damage and expression of pro-inflammatory cytokines and chemokines from infected monocytes/macrophages promote excessive immune cell infiltration and cytokine responses [16]. Plasma of individuals, who have recovered from COVID-19 is rich in immunoglobulins active against SARS-CoV-2, is being entertained as possible treatment option [17]. Another management strategy of COVID-19 is to calm cytokine storm through immunomodulation. It includes use of corticosteroids, administration of intravenous immunoglobulins (IVIG) and blockade of cytokines by IL-6 receptor antagonist as tocilizumab [18].

The current research is focused on antivirals like darunavir (DRV) and its derivatives relating to its molecular modeling and molecular dynamic simulation. The *in silico* work will be beneficial for the researches focusing on development of new and effective antivirals for treatment of SARS CoV-2 that is COVID-19.

EXPERIMENTAL

Analogues designing: Structure activity relationship (SAR) disclosed that the primary amine group of darunavir is involved in receptor binding [19]. Library of computational derivatives of darunavir were generated by modifying primary amine group. The 2D structures of derivatives of darunavir were designed and drawn on Marvin-stretch version 5.5 (Academic version) and saved as SDF format for further study.

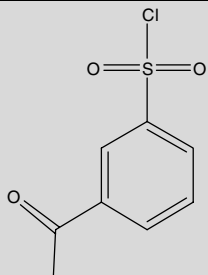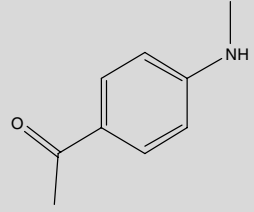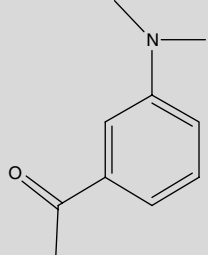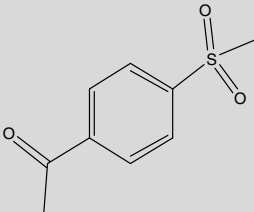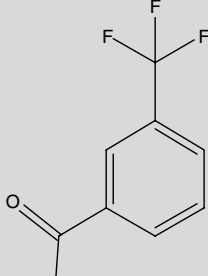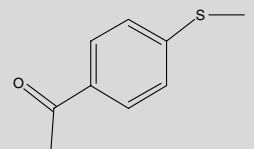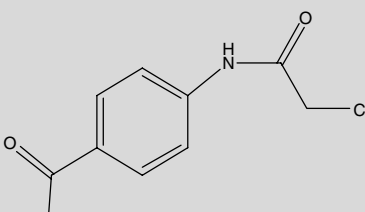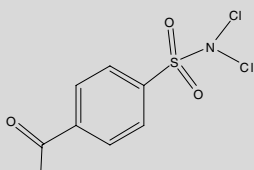**Preparation of inhibitor:** The energies of derivatives, co-crystal ligand and darunavir, were minimized by using Chem-Office Ultra (Chemical Structure Drawing Standard; Cambridge Soft Corporation, USA) through MMFF94X force field method and then converted into PDB format for further study. After that PDBQT files of compounds were created by MGL Tools (version 1.5.6) [20]. This conformation of compounds was further used for flexible docking method.

Preparation of protein: To predict the interactive model of designed derivatives with receptor of SAR-CoV-2, recently released protein (PDB: 6LU7) was selected [21] with resolution of 2.16 Å and downloaded from RCSB-PDB (http://www.rcsb.org/pdb/home/home.do). The co-crystal ligand, heteroatoms and water molecules were removed from selected protein using Discovery Studio Visualized (DSV). After that polar hydrogen and kollman united atom charges were added in receptor by utilizing Auto-Dock Tool (ADT) program.

Molecular docking: The molecular docking calculations were performed by AutoDock Vina using designed analogues and M^{pro} SARS-CoV protein model (PDB: 6LU7) whereas the co-crystallized ligand (N3) was redocked to evaluate the binding energy and orientation. The rectangular grid box was generated in the center of active site domain of M^{pro} with spacing between grid points was 0.636 Å and the dimension was -10.865 nm × 12.299 nm × 69.433 nm and size of the box was 44 Å × 46 Å × 46 Å. The docking study was performed by AutoDock Vina through a Lamarckian genetic algorithm (LGA). Default values of torsion angles, the number of generations and the energy evaluations were 7.5, 27000 and 2500,000, respectively.

Screening criteria: The best pose of docked model was evaluated by dlg file considering minimum value of ΔG score. Furthermore, hydrogen bonds, hydrophobic interaction and orientation of analogues in docked model were visualized by Discovery Studio Visualizer (DSV, BioVia, Discovery Studio Version 2.5, San Diego, USA), PyMol molecular visualization tool (The PyMOL Molecular Graphics System, version 2.0 Schrödinger, LLC), and protein ligand interaction profiler (PLIP) web server (Technical University of Dresden) [22].

Molecular dynamic simulations (MDS): It was evaluated that the analogues D8 and D15 showed minimum binding energy as compared to the other analogues, darunavir and co-crystal ligand (N3). That's why these were selected for MDS analysis to check out the stability of compounds at active site of receptor. The MDS was performed by Nanoscale Molecular Dynamics (NAMD) software package with CHARMM 36 force field [23]. Short MDS was performed for time period of 500 ps and 2fs time-steps were used for MDS through periodic boundary condition for all dimensions [24,25]. The constant temperature at 310 K using Langevin dynamics temperature and Langevin piston pressure method was used for constant pressure [26]. The particle-mesh Ewald (PME) method was used in the calculation of the electrostatic interactions with 10 Å non-bounded cutoff [27]. The structure and their trajectories were analyzed by Visual Molecular Dynamics (VMD) by means of backbone RMSD and αC (alpha carbon) fluctuations atom distances and their graph were plotted by Excel (version 2010). The hydrogen bond between ligand and protein, radius of gyration (Rg) and solvent accessible surface area (SASA) were also analyzed by VMD program.

Data analysis of MDS: The trajectory files were visualized by using VMD program and analyzed by αC (alpha carbon) fluctuations atom distances as well as protein backbone RMSD. Hydrogen bonds formed between polar atom of ligands and protein were also estimated and graph was plot by excel. Additionally, radius of gyration (Rg) and solvent accessible surface area (SASA) were examined. All graphs were plot in Microsoft excel.

RESULTS AND DISCUSSION

The primary amine group of darunavir was selected for the modification and converted into amide linkage (Table-1).

Structural activity relationship: Aromatic primary amine of darunavir has been selected for the modification. The acetophenone was added in primary amino group and produces amide linkage in D1 analogue. Due to this addition, the binding energy

TABLE-1
DESIGNED DERIVATIVES OF DARUNAVIR

Analogs	m.w.	m.f.	R	Analogs	m.w.	m.f.	R
D	547	$C_{27}H_{37}N_3O_7S$	H	D8	744	$C_{35}H_{42}N_3O_8SBr$	
D1	651	$C_{34}H_{41}N_3O_8S$		D9	700	$C_{35}H_{42}N_3O_8SCl$	
D2	756	$C_{41}H_{48}N_4O_8S$		D10	749	$C_{34}H_{40}N_3O_{10}S_2Cl$	
D3	697	$C_{35}H_{43}N_3O_8S_2$		D11	694	$C_{36}H_{46}N_4O_8S$	

D4	749	$C_{34}H_{40}N_3O_{10}S_2Cl$	
D5	694	$C_{36}H_{46}N_3O_8S$	
D6	719	$C_{35}H_{40}N_3O_8SF_3$	
D7	742	$C_{36}H_{43}N_4O_9SCl$	
D12	680	$C_{35}H_{44}N_4O_8S$	
D13	729	$C_{35}H_{43}N_3O_{10}S_2$	
D14	697	$C_{35}H_{43}N_3O_8S_2$	
D15	798	$C_{34}H_{40}N_4O_{10}S_2Cl_2$	

of compounds was somewhat increased. Furthermore, analogues of darunavir were divided into three groups according to the position of modification at incoming acetophenone group. In compounds D2 and D3 *ortho*-position of acetophenone were selected for the alteration and amino and sulfur groups were introduced, respectively. In case of compound D2, due to the addition of phenyl methanamine group, the binding energy further increased to -4.44 kcal/mol but when methyl sulfur was incorporated, the binding energy was reduced to -7.54 kcal/mol, which was considered as good. The *meta*-position of acetophenone was improved in second group of compounds (D4 to D6). Analogues D4, D5, and D6 were designed by the addition of sulfonyl chloride, tertiary amine and fluoroform, respectively, it was observed that by these additions, binding energies were decreased (-5.52 kcal/mol to -7.36 kcal/mol) that represents analogues were strongly bound with the SAR-CoV receptor. Analogue D6 showed highest energy among the member of second group. It may be due to the presences of fluoroform. Analogues D7 to D15 were included in the third group of compounds in which para position of acetophenone was altered and the binding score was reduced from -5.16 to

-9.85 kcal/mol. It was analyzed that upon the addition of methyl sulfonyl group, binding energy was increased to -5.92 kcal/mol and best binding affinity was developed in compounds D8, D10 and D15 by the addition of methyl bromide, sulfonyl chloride and dichloro sulfonamide, respectively. Furthermore, it was evaluated that among all, sulfur containing compounds that are D3, D4, D10, D13, D14 and D15 showed best binding energies and analogues having nitro group produced low to moderate scores. According to the binding energy, the best compound is D8, which has methyl bromide group at *para* position of upcoming acetophenone group. The darunavir and all derivatives have produced strong binding as compared to the co-crystal ligand (N3) of receptor.

Molecular docking study: The designed compounds and darunavir were bound with the active site of SARS-CoV receptor utilizing AutoDock tools. The binding energy, hydrogen bond and hydrophobic attraction are shown in Table-2 and the dlg files of docking complexes were used to predict the optimal pose by the help of binding energy and orientation of compounds at active site (Fig. 1). The co-crystal ligand (N3) was also redocked with the active site and observed binding energy was

TABLE-2
CHARACTERISTICS OF DARUNAVIR DERIVATIVES

Analogs	Binding energy	Number of hydrogen bonding	Amino Acid involve in H-bonding with bond length	Number of hydrophobic bond	Hydrophobic bonding	Other bonding
D	-7.92	2	141A LEU (2.41), 144A SER (2.9)	4	165A MET (3.21), 166A GLU (3.45), 168A PRO (3.97), 189A GLN (3.81)	
D1	-5.34	3	142A ASN (3.02), 166A GLU (2.08), 166A GLU (2.90)	4	141A LEU (3.78), 165A MET (3.95), 166A GLU (3.28), 189A GLN (3.89)	
D2	-4.44	1	166 A GLU (2.95)	2	165 A MET (3.94), 166A GLU (3.36)	SALT BRIDGE 163A HIS (3.86)
D3	-7.54	4	26A THR (1.96), 142A ASN (3.51), 166A GLU (2.01), 189A GLN (2.91)	1	189A GLN (3.73)	41A HIS 5.06 (π bond)
D4	-7.33	3	166A GLU (2.49), 166A GLU (2.96), 189A GLN (2.15)	3	166A GLU (3.61), 189A GLN (3.72), 189A GLN (3.74)	166A GLU 4.60 (SALT BRIDGE)
D5	-7.36	2	142A ASN (2.93), 142A ASN (2.03)	1	189A GLN (3.96)	166A GLU 5.20 (SALT BRIDGE)
D6	-5.52	2	140A PHE (1.94), 144A SER (3.03)			
D7	-7.1	4	166A GLU (2.33), 166A GLU (2.18), 189A GLN (2.88), 190A THR (3.02)	2	168A PRO (3.94), 191A ALA (3.92)	
D8	-9.85	3	142A ASN (2.72), 189A GLN (3.14), 189A GLN (3.16)	1	165A MET (3.42)	
D9	-6.66			6	165A MET (3.78), 168A PRO (3.91), 168A PRO (3.50), 168A PRO (3.13), 189A GLN (3.71), 189A GLN (3.87)	
D10	-8.28	3	41A HIS (2.69), 166A GLU (1.90), 166A GLU (2.48)	2	166A GLU (3.64), 189A GLN (3.87)	
D11	-6.57	3	166A GLU (2.62), 166A GLU (2.35), 166A GLU (3.18)	3	165A MET (3.46), 168A PRO (3.28), 168 PRO (3.45)	
D12	-5.92	2	166A GLU (1.85), 166A GLU (2.77)	1	168A PRO (3.98)	
D13	-5.16	3	166A GLU (2.51), 167A LEU (2.06), 191A ALA (3.05)			
D14	-7.46	3	166A GLU (2.22), 189A GLN (2.69), 189A GLN (3.00)	3	166A GLU (3.95), 168A PRO (3.66), 168A PRO (3.45)	
D15	-8.52	3	140A PHE (1.88), 142A ASN (3.12), 143A GLN (2.98)			
N3	-4.47	2	166A GLU (2.38), 166A GLU (2.58)	6	165A MET (3.42), 166A GLU (3.72), 168A PRO (3.56), 168A PRO (3.50), 169A THR (3.82), 189A GLN (4.00)	

only -4.47 kcal/mol. Darunavir showed good binding affinity with -7.92 kcal/mol score. All designed compounds were also evaluated for their binding energy and it was pragmatic that all compounds presented moderate to good binding energies that were in the range of -4.44 to -9.85 kcal/mol. Almost all compounds have produced up to 4 hydrogen bonds and up to 6 hydrophobic bonds.

Molecular dynamics simulation (MDS): On the basis of least binding energy, Two docking model were selected for the molecular dynamics simulation (MDS) study. The selected models were D8 and D15. The trajectories were examined by root mean square deviation (RMSD), root mean square fluctuation (RMSF), radius of gyration (Rg) and solvent accessible surface area (SASA). The results of above parameters were compiled in Fig. 2a-e.

The RMSD values of backbone atoms of protein of D8 and D15 docking models were evaluated to find out dynamic stabilities of the modelling models. The RMSD plot (Fig. 2a) of D8 and D15 docking models showed stable curves during 500ps simulation time. The results of RMSD were evidently
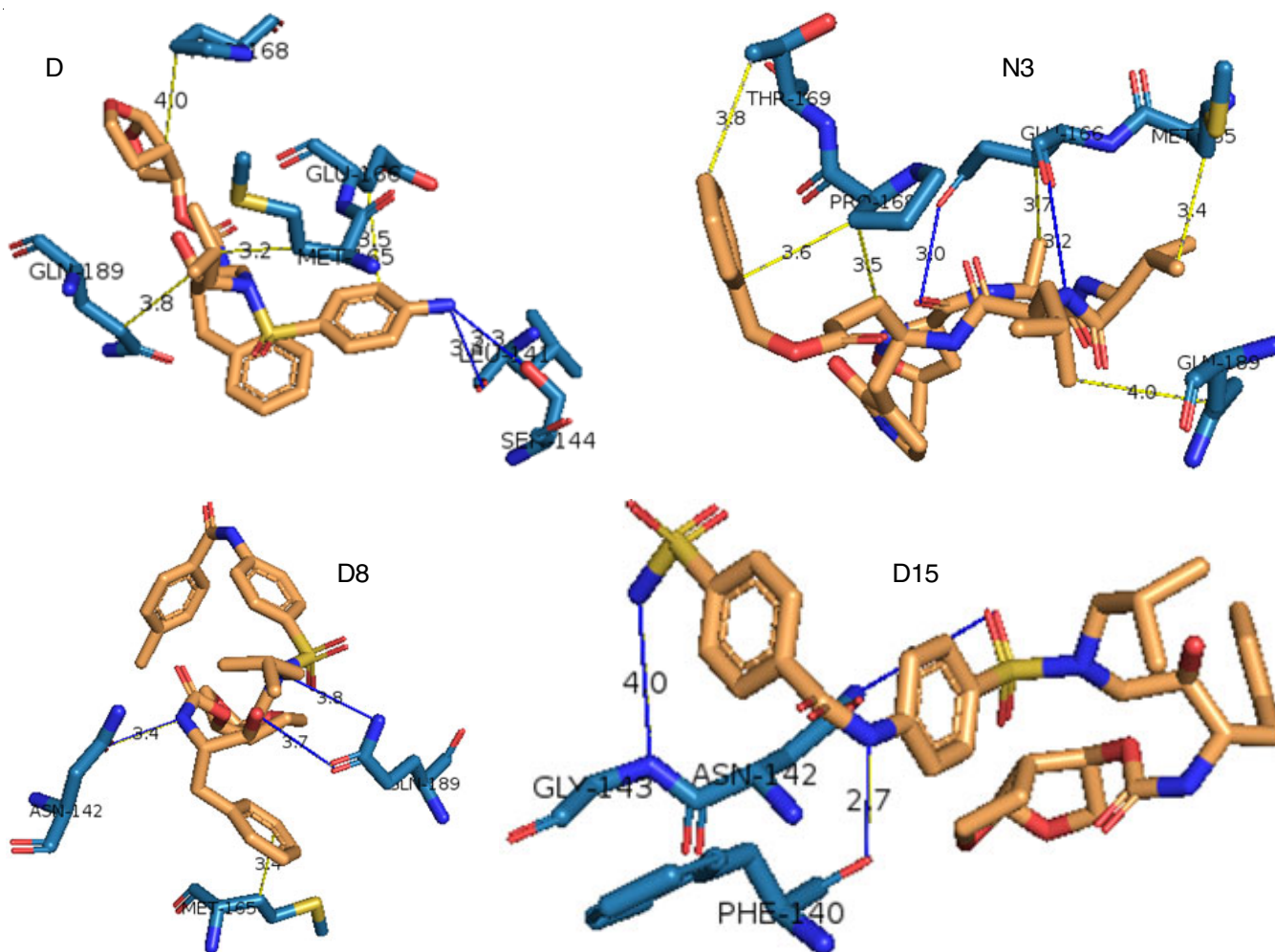
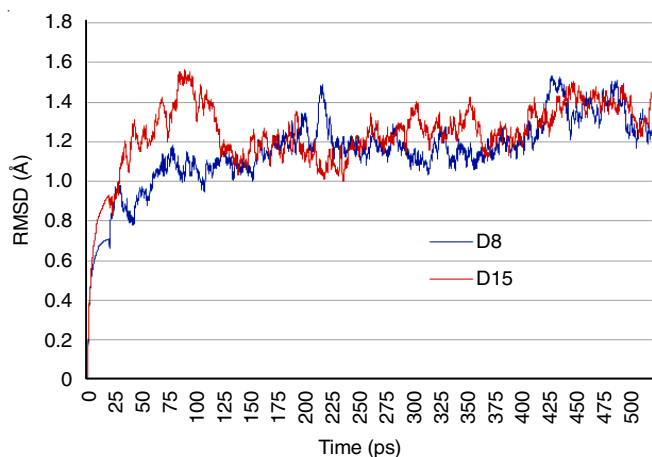Fig. 1. Schematic diagram of intermolecular interactions of protein and ligand

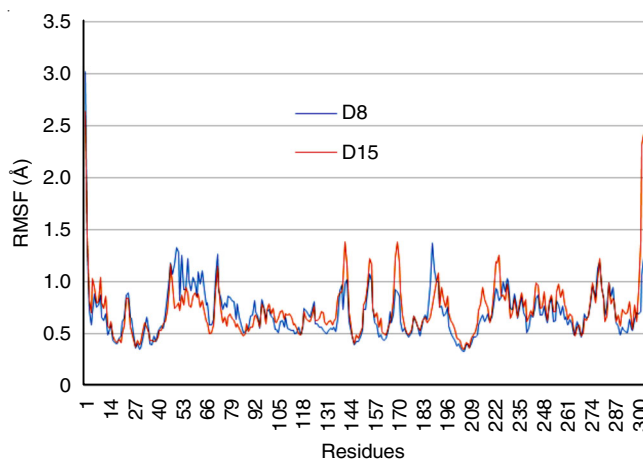Fig. 2a. RMSD of backbone atoms of protein with analog complex

Fig. 2b. RMS fluctuation of complexes D8 and D15

indicated that ligands were stable in pocket and do not change their orientation.

Furthermore, the result of fluctuation per residue were increased in two different regions in both selected models that are 40 to 60 and 140 to 190. It was analyzed that amino acid present in these region is involved in binding with ligand (Fig. 2b). The radius of gyration showed the density of protein system and no significant changes were detected in Rg values of D8, which was in the range of 21.92 to 22.71 and for D15, value was in the range of 21.93 to 22.81 (Fig. 2c). Similarly, the plot of SASA (Fig. 2d) also indicated the stability of docking complexes during simulation time. Moreover, the number of hydrogen bonds in MDS along 500ps verified the molecular docking results of the systems (Fig. 2e).
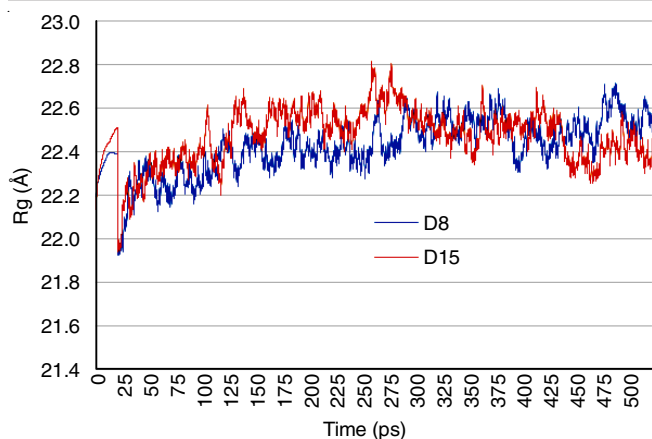
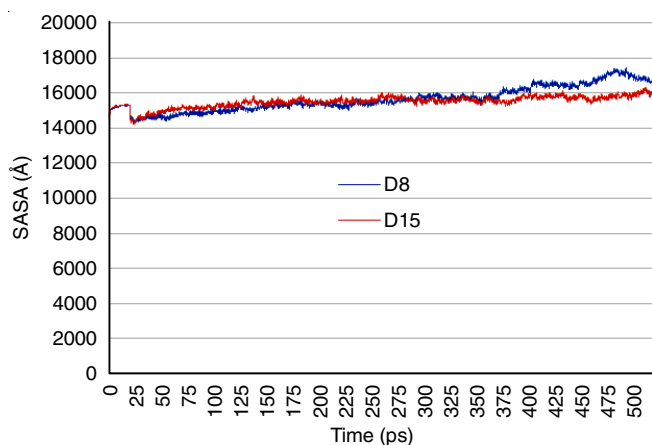Fig. 2c. Radius of gyration of complexes D8 and D15

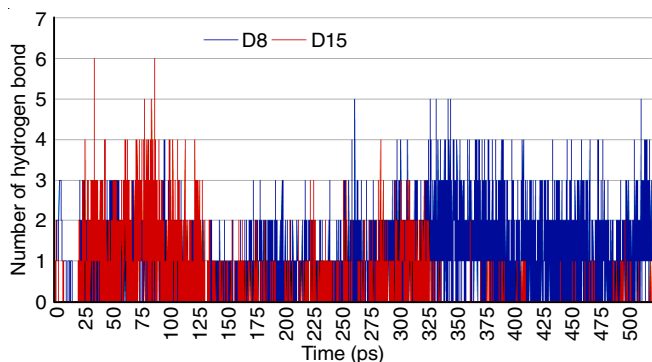Fig. 2d. Solvent accessible surface area of complexes D8 and D15

Fig. 2e. Hydrogen bonds of complexes D8 and D15

Conclusion

The present research study described the newly designed derivatives of darunavir and molecular docking with SARS-CoV-2 (PDB ID: 6LU7) using AutoDock Vina. The compounds were bound with amino acid present in active site that are Thr-26, His-41, Phe-140, Leu-141, Asn-142, Ser-144, Cys-145, His-163, Glu-166, Leu-167, Pro-168 and Gln-189. The binding energy of compounds were in the range of -4.44 to -9.85 kcal/mol. Analogs D8 and D15 were considered as best docked compounds and strongly bound with the receptor with least binding energy that is -9.85 kcal/mol and -8.52 kcal/mol respectively. The stability of best docked compounds were also

analyzed by mean of RMSD, RMSF, Rg and SASA and results indicated that the selected compounds were stable in binding pocket without changing the receptor native structures during 0.5 ns. The above selected analogues were considered as most active compounds with good stability and has potential for synthesis and development of the drug against corona virus.

CONFLICT OF INTEREST

The authors declare that there is no conflict of interests regarding the publication of this article.

REFERENCES

1. Z. Song, Y. Xu, L. Bao, L. Zhang, P. Yu, Y. Qu, H. Zhu, W. Zhao, Y. Han and C. Qin, *Viruses*, **11**, 59 (2019);
   https://doi.org/10.3390/v11010059
2. E.R. Gaunt, A. Hardie, E.C. Claas, P. Simmonds and K.E. Templeton, *J. Clin. Microbiol.*, **48**, 2940 (2010);
   https://doi.org/10.1128/JCM.00636-10
3. T.K. Cabeça, C. Granato and N. Bellei, *Influenza Other Respir. Viruses*, **7**, 1040 (2013);
   https://doi.org/10.1111/irv.12101
4. R.M. Anderson, C. Fraser, A.C. Ghani, C.A. Donnelly, S. Riley, N.M. Ferguson, G.M. Leung, T.H. Lam and A.J. Hedley, *Philos. Trans. R. Soc. Lond. B Biol. Sci.*, **359**, 1091 (2004);
   https://doi.org/10.1098/rstb.2004.1490
5. R. Channappanavar and S. Perlman, *Semin. Immunopathol.*, **39**, 529 (2017);
   https://doi.org/10.1007/s00281-017-0629-x
6. X. Yang, Y. Yu, J. Xu, H. Shu, J. Xia, H. Liu, Y. Wu, L. Zhang, Z. Yu, M. Fang, T. Yu, Y. Wang, S. Pan, X. Zou, S. Yuan and Y. Shang, *Lancet Respir. Med.*, **8**, 475 (2020);
   https://doi.org/10.1016/S2213-2600(20)30079-5
7. S. Tian, Y. Xiong, H. Liu, L. Niu, J. Guo, M. Liao and S.-Y. Xiao, *Mod. Pathol.*, **33**, 1007 (2020);
   https://doi.org/10.1038/s41379-020-0536-x
8. S. Shi, M. Qin, B. Shen, Y. Cai, T. Liu, F. Yang, W. Gong, X. Liu, J. Liang, Q. Zhao, H. Huang, B. Yang and C. Huang, *JAMA Cardiol.*, **5**, 802 (2020);
   https://doi.org/10.1001/jamacardio.2020.0950
9. J.F.-W. Chan, S. Yuan, K.-H. Kok, K.K.-W. To, H. Chu, J. Yang, F. Xing, J. Liu, C.C.-Y. Yip, R.W.-S. Poon, H.-W. Tsoi, S.K.-F. Lo, K.-H. Chan, V.K.-M. Poon, W.-M. Chan, J.D. Ip, J.-P. Cai, V.C.-C. Cheng, H. Chen, C.K.-M. Hui and K.-Y. Yuen, *Lancet*, **395**, 514 (2020);
   https://doi.org/10.1016/S0140-6736(20)30154-9
10. S. Felsenstein, J.A. Herbert, P.S. McNamara and C.M. Hedrich, *Clin. Immunol.*, **215**, 108448 (2020);
    https://doi.org/10.1016/j.clim.2020.108448
11. A. Savarino, J.R. Boelaert, A. Cassone, G. Majori and R. Cauda, *Lancet Infect. Dis.*, **3**, 722 (2003);
    https://doi.org/10.1016/S1473-3099(03)00806-5
12. D. Haydar, T.J. Cory, S.E. Birket, B.S. Murphy, K.R. Pennypacker, A.P. Sinai and D.J. Feola, *J. Immunol.*, **203**, 1021 (2019);
    https://doi.org/10.4049/jimmunol.1801228
13. C.J. Gordon, E.P. Tchesnokov, J.Y. Feng, D.P. Porter and M. Götte, *J. Biol. Chem.*, **295**, 4773 (2020);
    https://doi.org/10.1074/jbc.AC120.013056
14. J. Shuter, *Ther. Clin. Risk Manag.*, **4**, 1023 (2008);
    https://doi.org/10.2147/TCRM.S3285
15. Z.A. Abassi, K. Skorecki, S.N. Heyman, S. Kinaneh and Z. Armaly, *Am. J. Physiol. Lung Cell. Mol. Physiol.*, **318**, L1020 (2020);
    https://doi.org/10.1152/ajplung.00097.2020

16. C.Y. Cheung, L.L. Poon, I.H. Ng, W. Luk, S.-F. Sia, M.H. Wu, K.-H. Chan, K.-Y. Yuen, S. Gordon, Y. Guan and J.S.M. Peiris, *J. Virol.*, **79**, 7819 (2005);
https://doi.org/10.1128/JVI.79.12.7819-7826.2005

17. E.M. Bloch, S. Shoham, A. Casadevall, B.S. Sachais, B. Shaz, J.L. Winters, C. Van Buskirk, B.J. Grossman, M. Joyner, J.P. Henderson, A. Pekosz, B. Lau, A. Wesolowski, L. Katz, H. Shan, P.G. Auwaerter, D. Thomas, D.J. Sullivan, N. Paneth, E. Gehrie, S. Spitalnik, E.A. Hod, L. Pollack, W.T. Nicholson, L. Pirofski, J.A. Bailey and A.A.R. Tobian, *J. Clin. Invest.*, **130**, 2757 (2020);
https://doi.org/10.1172/JCI138745

18. X. Zhang, K. Song, F. Tong, M. Fei, H. Guo, Z. Lu, J. Wang and C. Zheng, *Blood Adv.*, **4**, 1307 (2020);
https://doi.org/10.1182/bloodadvances.2020001907

19. K.G. Šašková, M. Kozíšek, P. Rezáèová, J. Brynda, T. Yashina, R.M. Kagan and J. Konvalinka, *J. Virol.*, **83**, 8810 (2009);
https://doi.org/10.1128/JVI.00451-09

20. O. Trott and A.J. Olson, *J. Comput. Chem.*, **31**, 455 (2010);
https://doi.org/10.1002/jcc.21334

21. Z. Jin, X. Du, Y. Xu, Y. Deng, M. Liu, Y. Zhao, B. Zhang, X. Li, L. Zhang, C. Peng, Y. Duan, J. Yu, L. Wang, K. Yang, F. Liu, R. Jiang, X. Yang, T. You, X. Liu, X. Yang, F. Bai, H. Liu, X. Liu, L.W. Guddat, W. Xu, G. Xiao, C. Qin, Z. Shi, H. Jiang, Z. Rao and H. Yang, *Nature*, **582**, 289 (2020);
https://doi.org/10.1038/s41586-020-2223-y

22. S. Salentin, S. Schreiber, V.J. Haupt, M.F. Adasme and M. Schroeder, *Nucleic Acids Res.*, **43(W1)**, W443 (2015);
https://doi.org/10.1093/nar/gkv315

23. B.R. Brooks, C.L. Brooks III, A.D. Mackerell Jr., L. Nilsson, R.J. Petrella, B. Roux, Y. Won, G. Archontis, C. Bartels, S. Boresch, A. Caflisch, L. Caves, Q. Cui, A.R. Dinner, M. Feig, S. Fischer, J. Gao, M. Hodoscek, W. Im, K. Kuczera, T. Lazaridis, J. Ma, V. Ovchinnikov, E. Paci, R.W. Pastor, C.B. Post, J.Z. Pu, M. Schaefer, B. Tidor, R.M. Venable, H.L. Woodcock, X. Wu, W. Yang, D.M. York and M. Karplus, *J. Comput. Chem.*, **30**, 1545 (2009);
https://doi.org/10.1002/jcc.21287

24. W.L. Jorgensen, J. Chandrasekhar, J.D. Madura, R.W. Impey and M.L. Klein, *J. Chem. Phys.*, **79**, 926 (1983);
https://doi.org/10.1063/1.445869

25. A.D. MacKerell Jr., D. Bashford, M. Bellott, R.L. Dunbrack Jr., J.D. Evanseck, M.J. Field, S. Fischer, J. Gao, H. Guo, S. Ha, D. Joseph-McCarthy, L. Kuchnir, K. Kuczera, F.T.K. Lau, C. Mattos, S. Michnick, T. Ngo, D.T. Nguyen, B. Prodhom, W.E. Reiher, B. Roux, M. Schlenkrich, J.C. Smith, R. Stote, J. Straub, M. Watanabe, J. Wiórkiewicz-Kuczera, D. Yin and M. Karplus, *J. Phys. Chem. B*, **102**, 3586 (1998);
https://doi.org/10.1021/jp973084f

26. R.W. Pastor, B.R. Brooks and A. Szabo, *Mol. Phys.*, **65**, 1409 (1988);
https://doi.org/10.1080/00268978800101881

27. T. Darden, D. York and L. Pedersen, *J. Chem. Phys.*, **98**, 10089 (1993);
https://doi.org/10.1063/1.464397